JOURNAL OF MATERIALS SCIENCE 32 (1997) 6665–6670

Effect of thermal annealing on the microstructure of ytterbium-implanted silicon wafers

Y. YANG, H. CHEN*, Y. Q. ZHOU, F. H. LI
*Institute of Physics, Chinese Academy of Sciences, Beijing 100080, People's Republic of China, * and also Beijing Laboratory of Electron Microscopy, Beijing 100080, People's Republic of China*

Ytterbium-implanted Si(0 0 1) wafers annealed at different temperatures (800, 900, 1000 and 1200 °C) have been examined by means of cross-section transmission electron microscopy (XTEM) and electron diffraction. The results indicate that two layers of defects exist in the samples, one mainly includes microtwins and the other includes ytterbium precipitates. The distribution and morphology of the defects depend mostly on the thermal annealing: the higher the annealing temperature, the larger the size of the defects and the closer are the layers of defects to the wafer surface. High-resolution images show the different characteristics and details of the defects under various annealing conditions. The relation between microstructure and luminescence response is also discussed.

1. Introduction

In recent years, optical studies on rare-earth element implantation into semiconductors, such as silicon and III–V compounds, were reported by several authors [1–7], owing to the promising application of such compounds in optical fibre telecommunication engineering. Sharply structured photoluminescence bands resulting from internal intra-4f-shell transitions of the rare-earth ions were observed. It has been shown that the luminescence is only bound up with the lattice position of rare-earth ions in the host materials but independent of the substrate and environment temperature. In addition, the process of ion implantation generates a large number of defects and even an amorphous surface layer in the target material, hence a thermal treatment has to be performed in order to remove implant-induced defects and to make the doping atoms electrically active. In the case of a rare-earth element implanted in silicon, several reports show that after annealing most of the implants migrate to the silicon surface, which is sometimes referred to as "segregation" [8, 9], while those which occupy the lattice sites having tetrahedral symmetry remain unmoved. In order to obtain a high luminescence efficiency, one should prevent, as much as possible, optically active ions from escaping to the substrate surface. However, when the rare-earth element substitutes the atomic sites of the host material, a stress will be generated. In the course of the regrowth of silicon layers during thermal annealing, other defects will occur to release the stress, and the rare-earth element will move to the substrate surface. Because the photoluminescence is related to the site and environment of implanted ions in the host material, the microstructure of ion-implanted material is important for its luminescence properties.

In this work, the defect structure and precipitate formation in ytterbium-implanted silicon wafers annealed at different temperatures were studied by the diffraction contrast technique and high-resolution electron microscopy (HREM). The relation between microstructure and photoluminescence is also discussed.

2. Experimental procedure

Ytterbium ions with an energy of 350 keV and a dose of $\sim 10^{12}$ cm^{-2} were implanted into Si(0 0 1) wafers at room temperature. After implantation, the wafers were annealed at 800, 900, 1000 and 1200 °C, for about 10 min. The details of this process will be given elsewhere [10].

The specimens for XTEM observation were prepared by using the method described by Dupuy [11]. The wafer was sectioned into rectangular slabs, and two of these slabs were glued face to face with araldite to form a sample with a sandwiched structure. The sample was then cut into thin slices about 300 μm thick using a wire saw. The slices were mechanically ground and polished to a thickness of 30 μm and finally ion milled by Ar^+ at 4 kV. The cross-sectional specimens were examined with a H-9000NA analytical electron microscope operated at 300 kV and a JEM-200CX high-resolution electron microscope operated at 200 kV.

3. Results

The cross-section micrographs illustrating the defect distribution in ytterbium-implanted silicon samples after annealing under different thermal conditions are shown in Fig. 1. Fig. 1a–c correspond to the samples annealed at 800, 900 and 1000 °C, respectively.

0022–2461

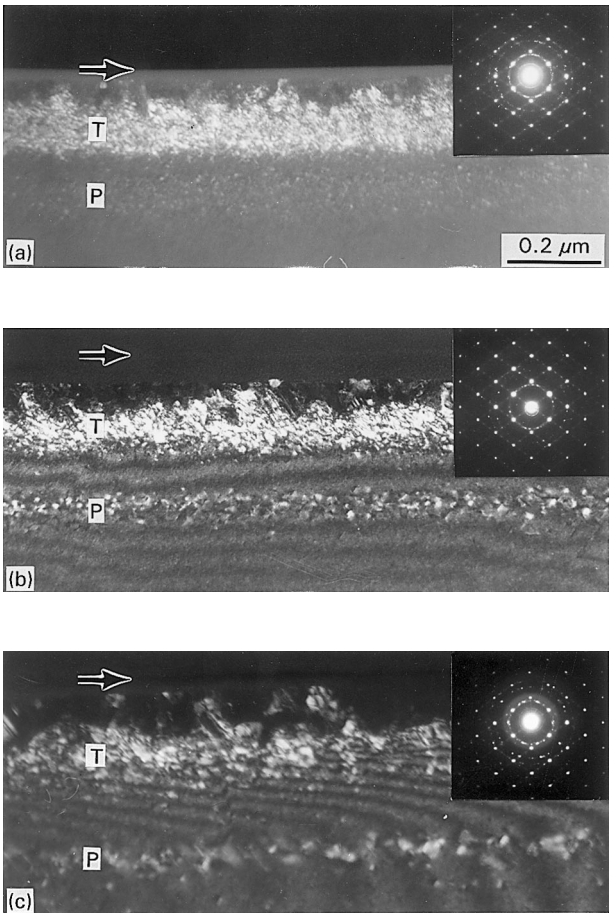

Figure 1 XTEM micrographs showing the defect distribution after annealing at (a) 800 °C, (b) 900 °C and (c) 1000 °C. The precipitates and microtwins are labelled P and T, respectively. Arrows indicate the wafer surface.

After annealing at 800 °C, two kinds of defects were produced in the silicon wafer. A layer with small microtwins (marked T) is located at a depth of 50–200 nm below the wafer surface, and a region containing many ytterbium precipitates (marked P), caused by the ion-implantation, appears beneath this layer. The precipitates are fine and scattered. The tiny precipitates and microtwins give rise to polycrystalline diffraction rings and diffraction streaks in the corresponding selected-area electron diffraction pattern (SAED) inset in Fig. 1a. The HREM image taken along the [1 1 0] orientation shows the characteristics of microtwins in the wafer treated at 800 °C (Fig. 2). The twins appear as small lamellae with an average dimension of about 3 nm, and intersection as well as overlapping of microtwins are frequently observed. These features of the defects imply that the grains in the sample are disordered to a certain extent.

From Fig. 1b, it can be seen that after annealing at 900 °C both the microtwins (or stacking faults) and the precipitates are apparently larger than those in the sample annealed at 800 °C. The features of the precipitates seen in this $\boldsymbol{g}_{2\,2\,0}$–$3\boldsymbol{g}_{2\,2\,0}$ weak-beam image show a contrast similar to the dislocation loops. However, such contrast is also visible in images corresponding to all reflections and turns into a solid dark contrast in all bright-field images formed with a deviation from the symmetrical illumination (not shown). The strong strain contrast observed within the loops implies that they are not dislocation loops or regions of faulted or twinned silicon. The absence of a $\boldsymbol{g}\cdot\boldsymbol{b} = 0$ criterion, the absorption contrast in weak-beam images and the strong inside–outside contrast at $\pm\boldsymbol{g}$, all indicate that

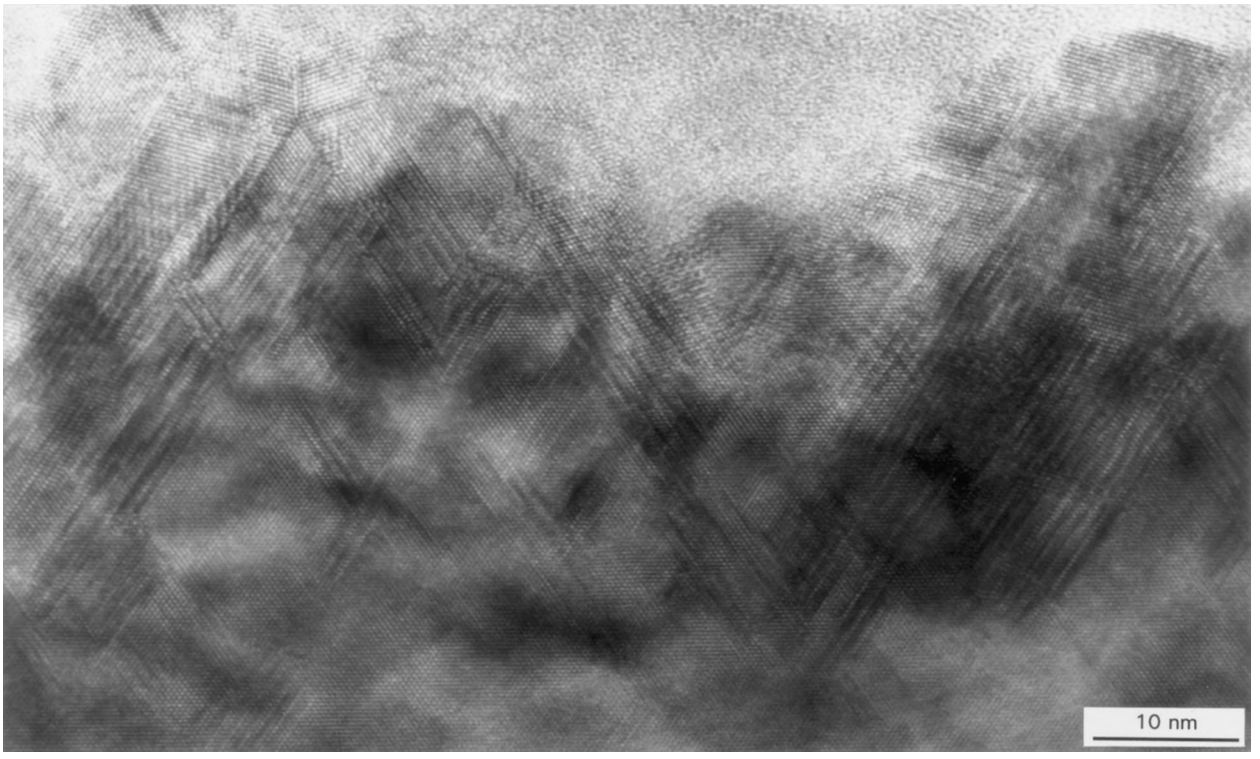

Figure 2 HREM image of the sample annealed at 800 °C taken with the incident beam parallel to the [1 1 0] direction. Microtwins can be seen.

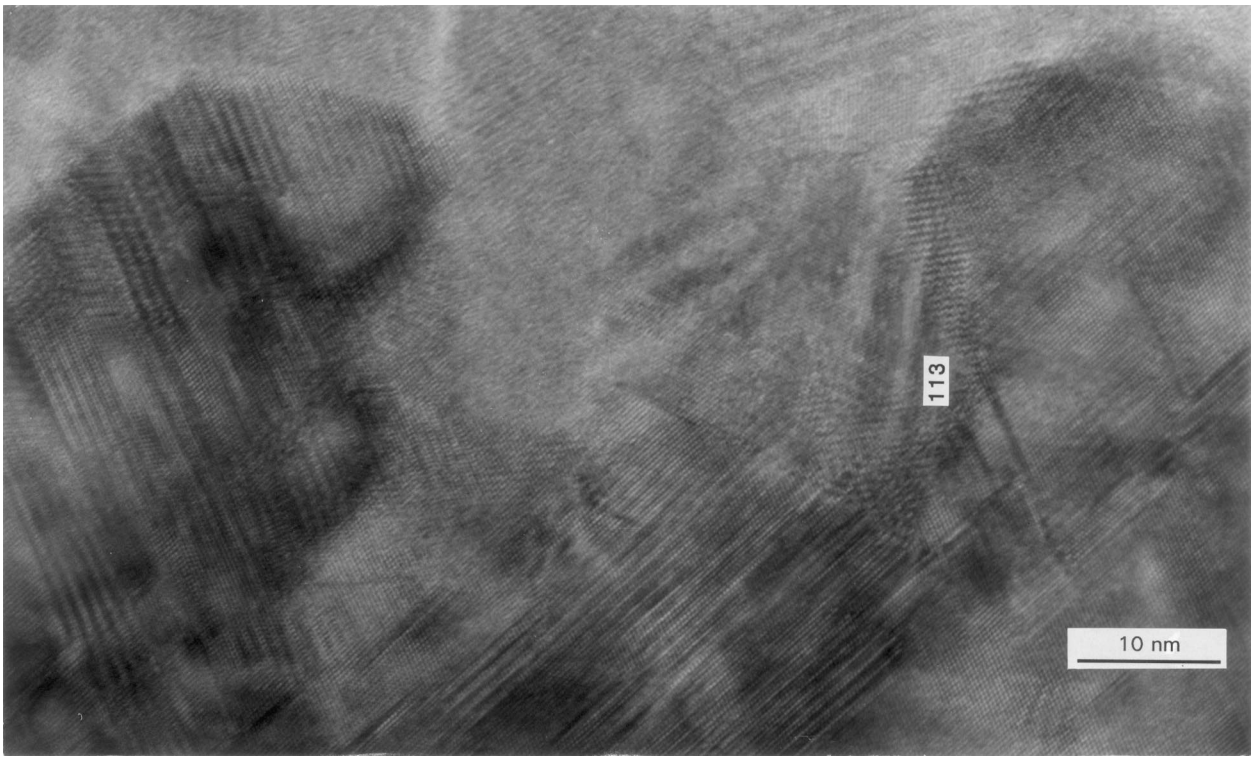

Figure 3 HREM image of the sample annealed at 900 °C taken with the incident beam parallel to the [1 1 0] direction showing the presence of microtwins and {1 1 3} stacking faults.

these defects are ytterbium-rich precipitates. Above the layer formed by these concentrated loop-like precipitates, a nearly defect-free epitaxially regrown layer is present. At a depth of about 40–190 nm beneath the wafer surface, there also exists a region of microtwins. The crystallinity of the sample becomes more perfect with the enlargement of the microtwins and precipitates. It is noticeable in the SAED pattern inset in Fig. 1b that both the diffraction streaks and the intensity of the polycrystalline rings become weaker.

Fig. 3 shows an HREM image taken for the same sample as Fig. 1b. Defects, such as twin regions containing about 30 lamellae and {1 1 3} stacking faults, are observed. {1 1 3} stacking faults are commonly present in ion-implanted silicon [12].

Similar to the wafers treated at 800 and 900 °C, microtwins and precipitates also exist in ytterbium-implanted silicon wafers annealed at 1000 °C (Fig. 1c). The morphologies of the defects seem sparse due to their continuous increase in size. Besides, it can be seen from Fig. 1c that the layer of the microtwins moves closely to the wafer surface and some of the ytterbium precipitates even spread into the twin layer. As can be seen in the HREM micrograph shown in Fig. 4, some ytterbium precipitates segregate just next to the "grown up" twins.

The phase of these precipitates can be identified by means of nano-beam electron diffraction as shown in Fig. 5. Fig. 5b is a schematic drawing which explains the electron diffraction pattern of Fig. 5a. It can be seen that the diffraction pattern of Fig. 5a is composed of two sets of diffraction spots. One is from the [1 1 0] zone of silicon which is represented by black spots together with indices 2 0 0, 1 1 1 and 1 $\bar{1}$ $\bar{1}$ in Fig. 5b, and the other is from the [1 0 0] zone of the precipitate YbSi. YbSi is orthorhombic in crystal structure with $a = 0.4178$ nm, $b = 1.031$ nm and $c = 0.3768$ nm. In Fig. 5b, the diffraction spots of the precipitate are represented by black crosses together with indices 0 0 2, 0 2 1 and 0 $\bar{2}$ 1.

All the above-mentioned results demonstrate that the distribution and morphologies of the defects in ytterbium-implanted silicon wafers are closely related to the annealing temperature. This is also consistent with the sample annealed at 1200 °C. As shown in Fig. 6, both the precipitates and microtwins have almost moved to the wafer surface, and their dimensions increased further. The nature of these microtwins was determined by comparing the micrographs taken under various diffraction conditions. Fig. 6a–c are images taken at the same region with the incident beam parallel to the [1 1 0] direction by using three different reciprocal vectors, $\boldsymbol{g}_{1\,1\,\bar{1}}$, $\boldsymbol{g}_{2\,2\,0}$ and $\boldsymbol{g}_{1\,1\,1}$, respectively. From the contrast change of the microtwins in Fig. 6a–c and from the criterion $\boldsymbol{g}\cdot\boldsymbol{R} = 3n$, it can be determined that most of the microtwins have translational vector, $\boldsymbol{R}$, of the type $\pm 1/3$ [1 1 1] or $\pm 1/3$ [$\bar{1}$ 1 1]. The electron diffraction pattern inset in Fig. 6 can then be indexed by means of these types of twinning and the matrix. For instance, the extra weak diffraction spots running along the [$\bar{1}$ 1 1] directions come from the 1/3($\bar{1}$ 1 1) and 1/3(1 $\bar{1}$ $\bar{1}$) twins, and similarly those along the [1 1 1] directions come from the 1/3(1 1 1) and 1/3($\bar{1}$ $\bar{1}$ $\bar{1}$) twins. The absence of polycrystalline diffraction rings implies better crystallinity.

The HREM image is also used for investigating the microtwins, as shown in Fig. 7. A triple periodicity region (labelled B) and a $\Sigma 9$ boundary [13] between twinned grains are present. The triple periodicity can

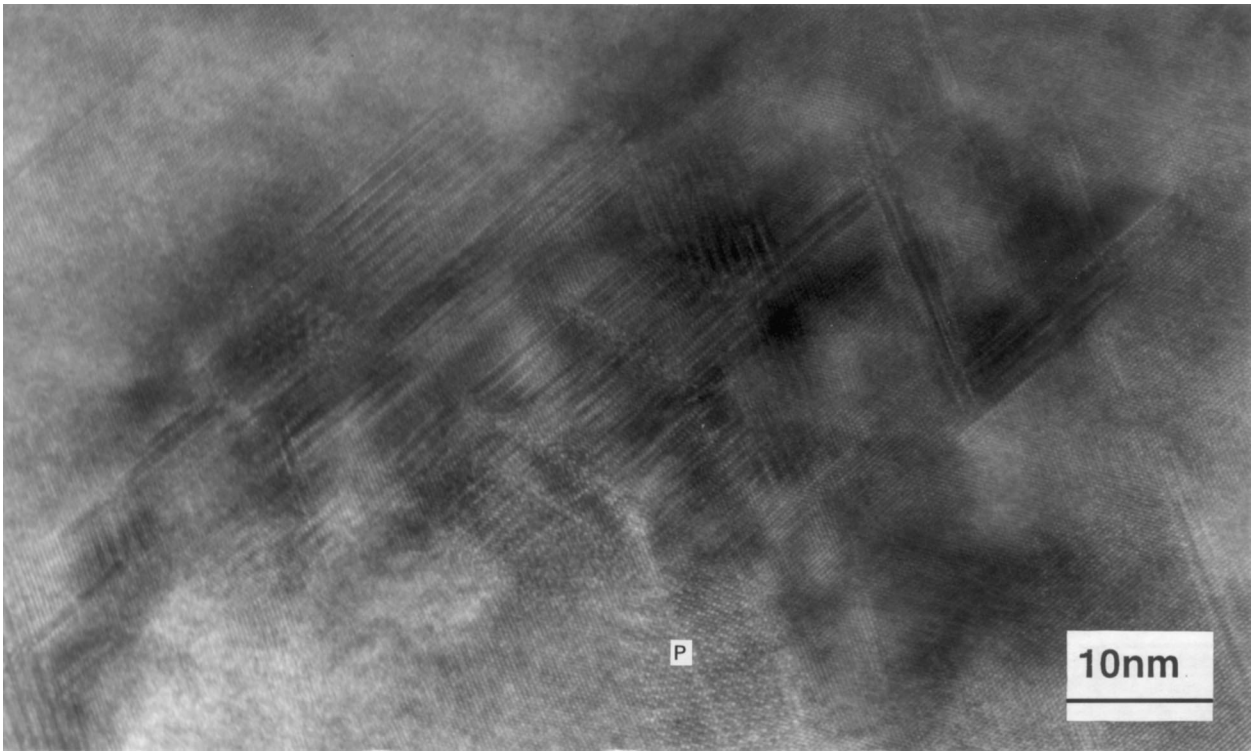

Figure 4 HREM image of the sample annealed at 1000 °C taken with the incident beam parallel to the [1 1 0] direction showing the precipitate segregation in the microtwin region.

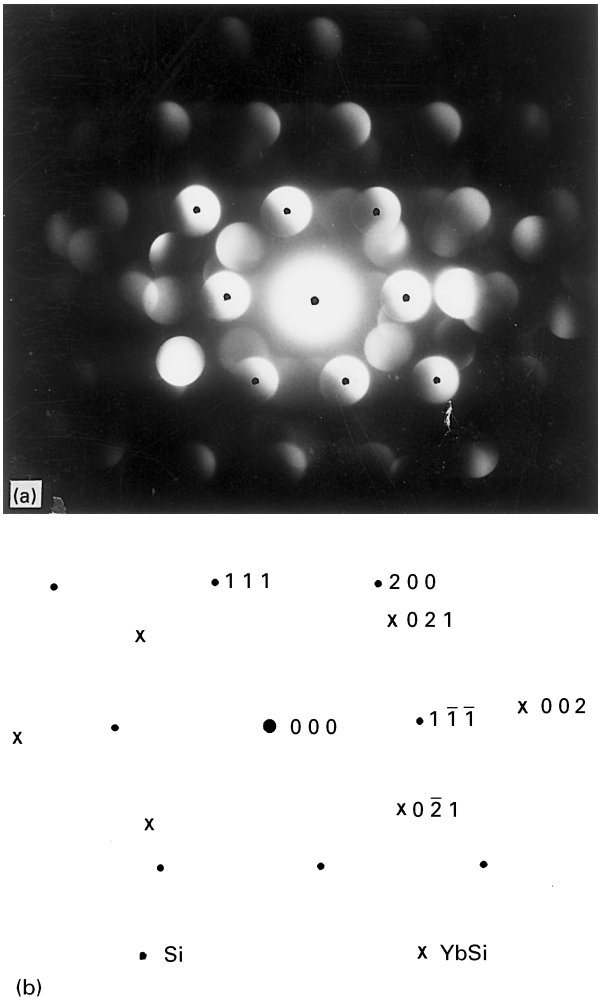

Figure 5 (a) Nano-beam electron diffraction pattern of the precipitates; (b) a schematic drawing of (a).

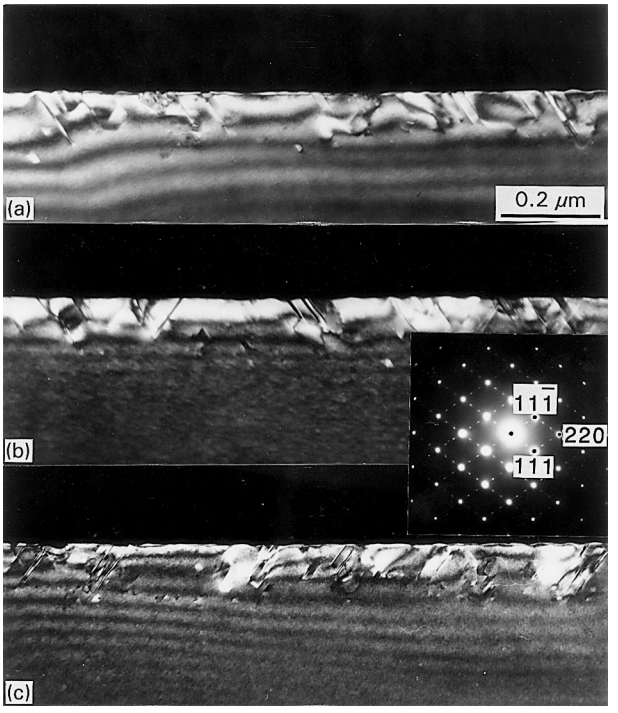

Figure 6 XTEM micrographs observed along the [1 1 0] direction showing a contrast change of the defects in the wafer treated at 1200 °C.

be explained by the overlap of two coherent twins extended from grains A and C mirrored to each other with the (1 1 1) plane parallel to the electron beam. The boundary between D and E shows a more complex pattern of extra bright dots. The coincidence sites in the overlap region between parts D and E produce the

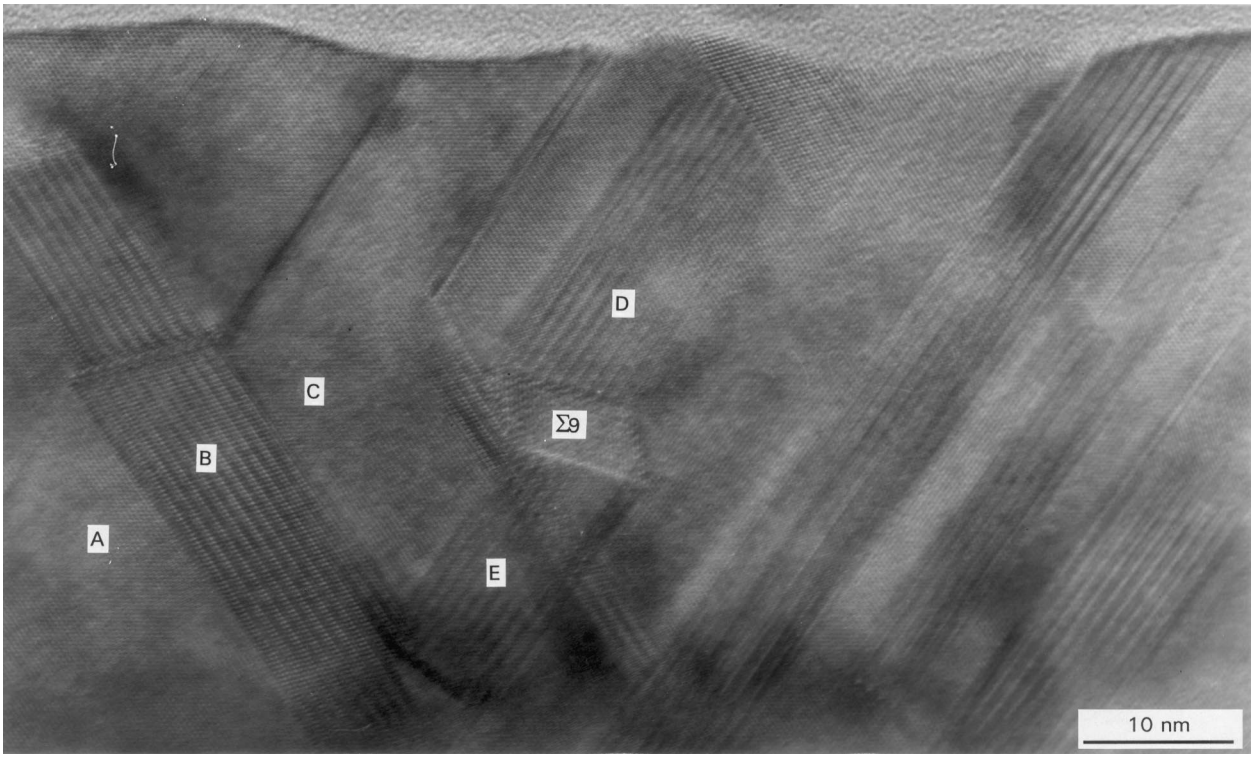

Figure 7 HREM image taken along the [1 1 0] direction showing the presence of a triple periodicity and a Σ9 boundary after annealing at 1200 °C.

two-dimensional lattice in direct space. The unit mesh is a parallelogram. It is an artificial two-dimensional 3×3 "superlattice" of the basic lattice. This is consistent with the fact that the two parts of the twin are related by a Σ9 coherent twin boundary.

4. Discussion

From the luminescence spectra detected by Li *et al.* [10], a weak Yb^{3+} luminescence intensity is observed in the sample annealed at 800 °C. As the annealing temperature is raised to 900 °C, the Yb^{3+} luminescence intensity increases sharply and it remains strong in the sample treated at 1000 °C. When the annealing temperature is above 1200 °C, no Yb^{3+} luminescence can be observed.

By comparing the luminescence spectra in all samples with the microstructures, it can be assumed that the luminescence efficiency is influenced by the site and environment of ytterbium precipitates in silicon wafers. In order to have good luminescence properties, it seems that the precipitates must be embedded into a more or less perfect epitaxial material, because in such a case the incomplete 4f electrons are screened by the outer filled $5s^2 5p^2$ orbitals, and hence they are only slightly affected by the crystalline environment [5]. It should be remarked that for the two defect regions formed in the ytterbium-implanted silicon, the luminescence efficiency depends mostly on the situation of the precipitate layer. Although ytterbium precipitates exist also in the microtwin layer, which are difficult to distinguish in the XTEM micrograph because of the strong contrast of microtwins, surrounded by defects, they hardly contribute to the luminescence efficiency, as in the case of the sample annealed at 1200 °C. In the wafer treated at 800 °C, the luminescence property is poor because the annealing temperature is so low that the silicon is poorly recrystallized and the ytterbium precipitate particles are too small. In the case of annealing at 900 and 1000 °C, the sample recrystallizes more or less perfectly, and in the meanwhile the migratation of implanted ytterbium to the wafer surface is suppressed. This leads to a better luminescence property. Therefore, a larger size of ytterbium precipitates is possibly beneficial to the improvement of luminescence.

5. Conclusion

The microstructure of ytterbium ion-implanted silicon wafers is strongly affected by thermal annealing. In all the examined samples the implant-related defects, which arise upon annealing, mainly include ytterbium precipitates and microtwins. The precipitates are characterized by means of nano-beam electron diffraction as YbSi and the type of the microtwins was determined to be 1/3(1 1 1). High-resolution images reveal the detailed structure of the defects formed under various thermal annealing conditions. With increasing annealing temperature the crystallinity becomes more perfect, and meanwhile the defects increase in size and move gradually to the wafer surface.

References

1. W. H. HAYDL, H. D. MULLER, H. ENNEN, W. KORBER and K. W. BENZ, *Appl. Phys. Lett.* **46** (1985) 870.
2. Y. S. TANG, K. C. HEASMAN, W. P. GILLIN and B. J. SEALY, *ibid.* **55** (1989) 432.

3. Y. S. TANG and J. P. ZHANG, *J. Crys. Growth* **102** (1990) 681.
4. Y. S. TANG and B. J. SEALY, *J. Appl. Phys.* **68** (1990) 2530.
5. H. ENNEN, G. POMRENKE and A. AXMANN, *ibid.* **57** (1985) 2182.
6. H. ENNEN, J. WAGNER, H. D. MULLER and R. S. SMITH, *ibid.* **61** (1987) 4877.
7. D. J. EAGLESHAM, J. MICHEL, E. A. FITZGERALD, D. C. JACOBSON, J. M. POATE, J. L. BENTON, A. POLMAN, Y. H. XIE and L. C. KIMERLING, *Appl. Phys. Lett.* **58** (1991) 2797.
8. A. POLMAN, J. S. CUSTER, E. SNOEKS and G. N. van den HOVEN, *ibid.* **62** (1993) 507.
9. J. S. CUSTER, A. POLMAN and H. M. van PINXTEREN, *J. Appl. Phys.* **75** (1994) 2809.
10. D. X. LI, H. CHEN, et al. to be published.
11. M. DUPUY, *J. Microsc. Spectrosc. Electron.* **9** (1984) 163.
12. Z. L. WANG, B. X. ZHANG, Q. T. ZHAO, Q. LI, J. R. LIEFTING, R. J. SCHREUTELKAMP and F. W. SARIS, *J. Appl. Phys.* **71** (1992) 3780.
13. H. BENDER, A. De VEIRMAN, J. VAN LANDUYT and S. AMELINCKX, *Appl. Phys. A* **39** (1986) 83.

Received 20 February
and accepted 1 December 1995